Key Engineering Materials Vols. 206-213 (2002) pp 1457-1460
Online available since 2001/Dec/15 at www.scientific.net

doi:10.4028/www.scientific.net/KEM.206-213.1457

Sintering and Grain Size Influence on the Electrical Properties of the $Bi_{26}Mo_9WO_{69}$ Ceramics

F. C. Fonseca[1], M.C. Steil[2], R.N. Vannier[2], R. Muccillo[1]

[1] Instituto de Pesquisas Energéticas e Nucleares, Comissão Nacional de Energia Nuclear, C.P. 11049, Pinheiros, 05422-970, S. Paulo, SP, Brazil.

[2] Laboratoire de Cristallochimie et Physicochimie du Solide (UPRES A 8012), ENSCL, BP 108, 59652 Villeneuve d'Ascq cedex, France.

Keywords: Bismuth-based material; Microstructure; Impedance spectroscopy; Electrical properties

Abstract. In the field of oxide ion conduction, bismuth-based materials exhibit interesting electrical properties at moderate temperatures: 300 °C - 600 °C. The $Bi_{26}Mo_{10-x}W_xO_{69}$ solid solution is a one-dimensional ion conductor with a structure based on $[Bi_{12}O_{14}]_\infty$ columns. The sintering behaviour of the $Bi_{26}Mo_9WO_{69}$ powder was studied by dilatometric analysis. In order to investigate the influence of the microstructure on the electrical properties of the $Bi_{26}Mo_9WO_{69}$ ceramics, dense samples with different grain sizes were produced by isostatic pressing and controlling sintering temperature and time. The electrical properties were studied by impedance spectroscopy. Impedance spectroscopy results show that the electrical conductivity depends on the microstructural properties, remarkably on the grain size.

1. Introduction

In the field of oxide ion conduction, bismuth-based materials exhibit interesting electrical properties at moderate temperatures: 300 °C - 600 °C. Depending on their dimensionality, they can be classified into three groups: three-dimensional ion conductors, Bi_2O_3 being the prototype of the bismuth-based oxides [1]; two-dimensional ion conductors represented by the BIMEVOX family, which has generated an increasing interest during the last decade [2]; one-dimensional ion conductors, with $Bi_{26}Mo_{10}O_{69}$ and related phases, with a structure based on $[Bi_{12}O_{14}]_\infty$ columns [3].

Depending on the temperature, $Bi_{26}Mo_{10}O_{69}$ exhibits *two polymorphs: a triclinic form, stable from room temperature to 310 °C, and a monoclinic one, stable above 310 °C up to the melting point (~ 975 °C).* The triclinic distortion at room temperature is very small and the $Bi_{26}Mo_{10}O_{69}$ structure was resolved in $P_{2/c}$ space group with a = 11.742 (8) Å, b = 5.800 (7) Å, c = 27.77 (5) Å and β = 102.94 (6)° from single crystal X-ray diffraction data [3]. In order to improve the electrical properties of this phase, several attempts of substitution for bismuth or molybdenum were performed [4]. The best properties were obtained for tungsten-doped phases. A $Bi_{26}Mo_{10-x}W_xO_{69}$ solid solution with $0 \le x < 2$ was evidenced. An electrical conductivity value of 10^{-3} S.cm^{-1} was measured at 350 °C with a thermal activation energy of 0.43 eV in the monoclinic domain [4]. These materials are potentially attractive for use as electrolytes in some devices such as oxygen generators. For this application a compactness higher than 95% is required [5]. Therefore, to have usable dense ceramics, the sintering conditions have to be optimized.

The effect of grain size on electrical properties is well known. Impedance spectroscopy has become an important technique to study electrical properties of materials, and today it is a standard technique for solid electrolyte characterization. Many efforts trying to correlate the electrical properties to the microstructural properties using impedance spectroscopy have been reported: grain growth and pore elimination during sintering of yttria-stabilized zirconia [6-8]; dependence of the electrical properties on grain size of BICOVOX [9]; and the powder synthesis technique effect on the electrical conductivity of LSGM [10].

In this study, the $Bi_{26}Mo_9WO_{69}$ composition was selected. In a first step, the sintering behavior was studied; in a second step, the influence of the microstructure on the electrical properties were examined. A complete investigation about the phase transition, electrical properties and microstructure relationships in this material was published elsewhere [11].

2. Experimental

The $Bi_{26}Mo_9WO_{69}$ powder was prepared by solid state reaction in air from stoichiometric amounts of Bi_2O_3 (Riedel-De-Haën, 99.5% purity, previously decarbonated at 600°C), MoO_3 (Merck, 99.5%) and WO_3 (Riedel-De-Haën, 99%), as previously described [3]. The obtained powder was attrition milled (Netzsch PE 075) with zirconia to reduce the mean particle size. The milling conditions were: 30 wt% of $Bi_{26}Mo_9WO_{69}$ in a suspension of ethanol, 1000 rpm, for 4 h. The resulting powder was analyzed by SEM and the estimated average particle size was smaller than 1 μm. The sintering behavior was studied by dilatometric analysis (Linseis dilatometer) with 10 °C/min heating rate, 900 °C maximum temperature, 1 h holding time at maximum temperature and 10 °C/min cooling rate in air.

Cylindrical pellets (10 mm diameter and approximately 4 mm thickness) were prepared by uniaxial pre-pressing followed by isostatic pressing at 150 MPa. The average green density was 57.3 ± 0.7 % TD (theoretical density = 7.63 g/cm^3 [4]). A $Bi_{26}Mo_9WO_{69}$ powder bed inside an alumina crucible was used for sintering in a resistive furnace. In order to obtain different average grain sizes, sintering temperatures ranged from 750 °C to 900 °C and sintering time of 1 h. Heating and cooling rates were 10 °C/min. Three supposedly identical samples of each different sintering temperature were produced for evaluation of experimental dispersion of density determinations. Final typical dimensions were 7 mm in diameter and 3 mm thick. Polished and thermally etched samples were observed in a Jeol JSM5300 scanning electron microscope for microstructural characterization. Grain boundaries were revealed by thermal etching at 50 °C (or 100 °C depending on sintering temperature) below the sintering temperature for 20 min..

The electrical properties were studied by impedance spectroscopy with a computer controlled Solartron 1260 impedance analyzer with 1 V amplitude signal over the 1 Hz to 30 MHz frequency range. Gold electrodes were applied to the parallel surfaces of the samples by sputtering. Impedance measurements were performed in three consecutive heatings between 200 °C and 500 °C in air. The curve fitting was done with the ZView (Impedance / Gain Phase Graph analysis software – Scribner Associates Inc.).

3. Results and discussion

3.1- Sintering behaviour and sample microstructure

Fig. 1 shows the dilatometric curve for $Bi_{26}Mo_9WO_{69}$. The shrinkage starts at approximately 550 °C and the sintering process finishes at about 830 °C with a final shrinkage of approximately 17%. The Samples sintered for 1h at temperatures between 750 °C and 900 °C reach the maximum relative density values (around 96.5 %).

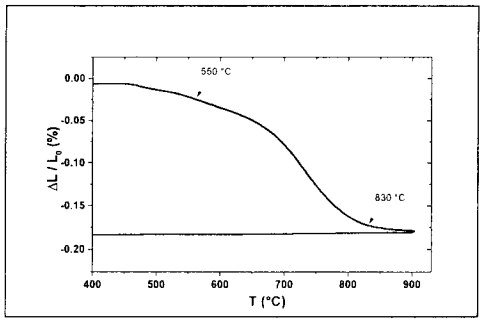

Fig. 1: Shrinkage curve as a function of the temperature for $Bi_{26}Mo_9WO_{69}$ powder

Fig. 2 shows the micrographs corresponding to samples sintered at 750 °C , 850 °C, 900 °C. A first observation shows that the specimens are dense with low intergranular porosity. An increase of grain size with increasing sintering temperature and time is noticed. The estimated average grain size for the sample sintered at 750 °C / 1 h is about 1 μm and for the sample sintered at 900°C / 1 h is about 10 μm. Samples sintered at 750 °C are more homogeneous than samples sintered at higher temperatures, which show abnormal grain growth.

3.2- Electrical properties

Fig. 3 shows impedance diagrams measured at several temperatures of samples with different sintering temperatures.

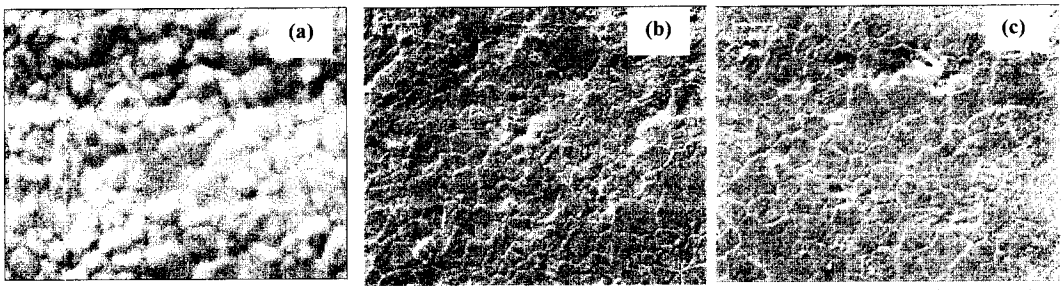

Fig.2 : Scanning electron micrographs of $Bi_{26}Mo_9WO_{69}$ specimens sintered at (a) 750 °C, (b) 850 °C and (c) 900 °C.

An evolution of the shape of the impedance diagrams can be observed as a function of the measuring temperature (in the phase transition temperature range) and sintering conditions. It is characterised by two main features: the decrease of the total electrical resistivity and a progressive distortion towards a two semicircles shape.

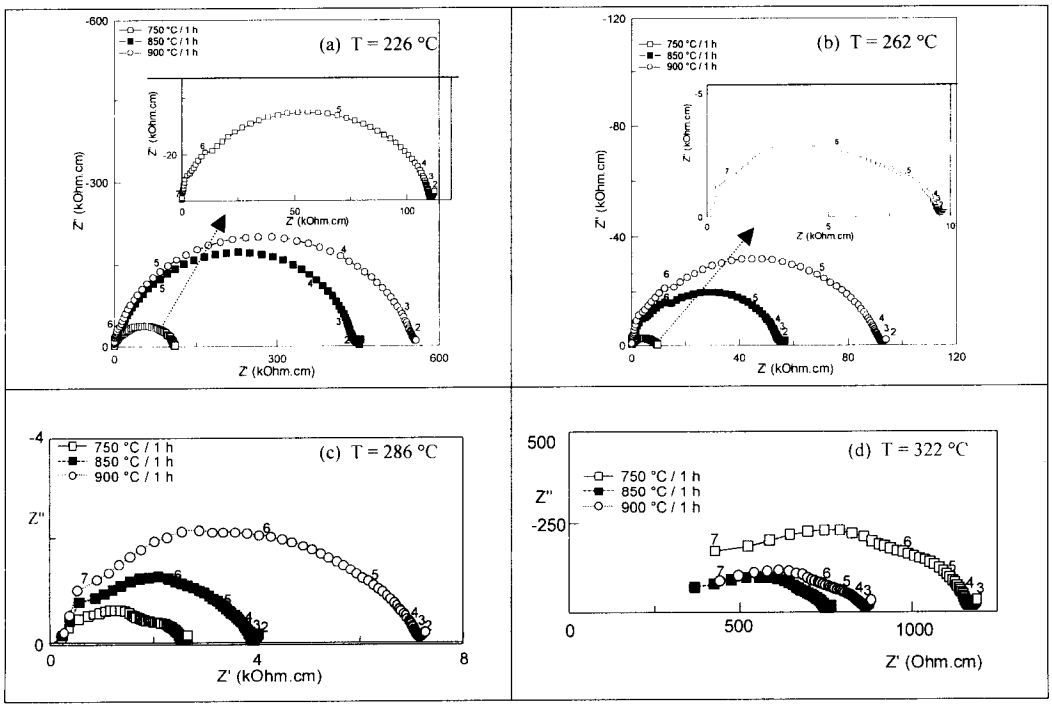

Fig. 3 : Impedance diagrams of $Bi_{26}Mo_9WO_{69}$ specimens measured at 226 °C, 262 °C, 286 °C and 322°C. The numbers 2, 3, 4,...,7 indicate the logarithm of signal frequency.

Several conclusions can be drawn from the diagrams. At low temperatures (Fig. 3a) all samples show only one semicircle with calculated capacitance values around $8x10^{-12}$ F. An increase of the total resistivity with sintering temperature (which is directly related to the microstructure evolution shown in Fig. 2): 112 and 500 kΩ.cm for samples sintered at 750 °C and 900 °C, respectively. Specimens *sintered at 750 °C are less resistive before phase transition (T < 300 °C).* Samples sintered at temperatures higher than 750 °C show a rapid decrease of the total electrical resistivity, that starts at approximately 260 °C. This decrease is observed to happen at lower temperatures for samples sintered at 800 °C and 850 °C (with intermediary grain sizes) than in samples sintered at 900 ° C (Fig. 3b and c). *After phase transition the samples sintered at 750 °C have larger resistivities than the all sintered at higher temperatures* (Fig. 3d). Specimens sintered at 750 °C clearly exhibit two semicircles for temperatures higher than approximately 260 °C that are

most probably related to the intragranular properties and intergranular blocking of charge carriers, since they have the higher grain boundary density (smaller grain size) [12-14]. All specimens sintered at 800 °C and higher temperatures show highly distorted semicircles during the phase transition (Fig. 3c) and two semicircles are identified for temperatures above the phase transition (Fig. 3d).

In the triclinic domain *(low temperature)* only one semicircle was observed. A possible interpretation is that the triclinic, monoclinic and the grain boundary contributions overlap, with the triclinic response in the middle. After the phase transition, the triclinic response vanishes and it is possible to separate out the monoclinic bulk and grain boundary relaxations.

Fig. 4 shows Arrhenius plots of the total electrical conductivities of the studied samples.

Two distinct groups can be distinguished: specimens sintered at 750 °C and specimens sintered at higher temperatures. The specimens sintered at 750 °C exhibits a continuous transition of the electrical conductivity values close to the phase transition temperature. The specimens sintered at higher temperatures are less conductive at temperatures below 280 °C and the electrical conductivity values increase rapidly in the 260 °C - 280 °C range. For temperatures above 300 °C the electrical conductivity values are of the same order of magnitude for all sintering temperatures. The average activation energy values calculated for the triclinic and monoclinic phases, taking into account all sintering temperatures, are 1.1 ± 0.1 eV and 0.48 ± 0.04, respectively.

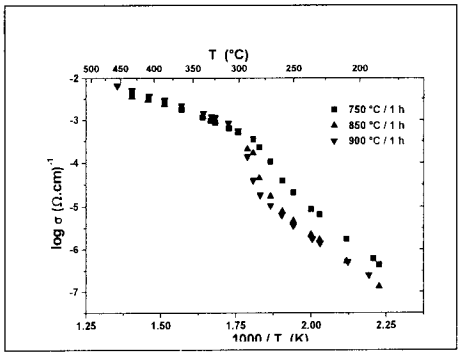

Fig. 4: Arrhenius plots of the total electrical conductivities of the studied samples.

Conclusion

Using reactive $Bi_{26}Mo_9WO_{69}$ ceramic powders, prepared by solid state reaction and attrition milling, specimens were obtained by sintering at relatively low temperature (750 °C) with relative density upper to 96 % of the theoretical density. Specimens with different average grain sizes were produced by varying the sintering temperature. In the high temperature monoclinic domain, the dependence of the impedance spectroscopy results on the microstructure is negligible. However, in the low temperature triclinic domain, the electrical properties are clearly dependent upon the microstructure: specimens with small grain sizes keep the monoclinic phase (more conductive) down to temperatures lower than those with relatively larger grain sizes

References

[1] T. Takahashi, H. Iwahara, Y. Nagai: J. Electrochem. Soc. Vol. 117 (1970), pp. 244.
[2] F. Abraham, J. C. Boivin, G. Mairesse, G. Nowogrocki: Solid State Ionics Vol. 40-41 (1990), pp. 934.
[3] R. N. Vanier, G. Mairesse, F. Abraham, G. Nowogrocki:, J. Solid State Chem.Vol. 122 (1996), pp. 394.
[4] R. N. Vanier, S. Danzé, G. Nowogrocki, Huvé, G. Mairesse: Solid State Ionics Vol. 136-137 (2000), pp. 51.
[5] B. Steele: C. R. Acad. Sci. Paris, t.1, serie IIc (1998), pp. 533.
[6] D. Z. de Florio, R. Muccillo: Solid State Ionics Vol. 123 (1999), pp. 301.
[7] M. C. Steil, F. Thevenot, M. Kleitz: J. Electrochem. Soc. Vol.144 (1997), pp. 390.
[8] S. P. S. Badwal: Solid State Ionics Vol.76 (1995), pp. 67.
[9] M. C. Steil, J. Fouletier, M. Kleitz, P. Labrune: J. European Ceram. Soc.Vol. 19 (1999), pp. 815.
[10] K. Huang, M. Feng, J. B. Goodenough: J. Amer. Ceram. Soc. Vol. 79 (1996), pp. 1100.
[11] F. C. Fonseca, M.C. Steil, R.N. Vannier, G. Mairesse, R. Muccillo : Solid State Ionics Vol. 140 (2001) pp. 161.
[12] A. I. Ioffe, M. V. Inozemtzev, A. S. Lipilin, M. V. Perfilev, S. V. Karpachov: Phys. Stat. Sol. (a) Vol. 30 (1975), pp. 87.
[13] S. H. Chu, M. A. Seitz: J. Solid State Chem. Vol. 23 (1978) pp. 287.
[14] M. J. Verkerk, B. J. Middelhuis, A. J. Burggraaf: Solid State Ionics Vol. 6 (1982) pp.159.

Euro Ceramics VII
doi:10.4028/www.scientific.net/KEM.206-213

Sintering and Grain Size Influence on the Electrical Properties of the Bi₂₆Mo₉WO₆₉ Ceramics
doi:10.4028/www.scientific.net/KEM.206-213.1457